INT. J. REMOTE SENSING, 10 JUNE, 2004,
VOL. 25, NO. 11, 2015–2036

Taylor & Francis
Taylor & Francis Group

Early damaged area estimation system using DMSP-OLS night-time imagery

M. KOHIYAMA

Institute of Industrial Science, The University of Tokyo, 4-6-1 Komaba, Meguro-ku, Tokyo 153-8505, Japan; e-mail: kohiyama@iis.u-tokyo.ac.jp

H. HAYASHI, N. MAKI, M. HIGASHIDA

Earthquake Disaster Mitigation Research Center, National Research Institute for Earth Science and Disaster Prevention, 4F Human Renovation Museum 1-5-2 Kaigan-dori, Wakihama, Chuo-ku, Kobe, Hyogo 651-0073, Japan

H. W. KROEHL, C. D. ELVIDGE

NOAA National Geophysical Data Center, 325 Broadway Boulder, Colorado 80303, USA

and V. R. HOBSON

Cooperative Institute for Research in Environmental Sciences, University of Colorado, Boulder, Colorado 80303, USA

(*Received 4 July 2002; in final form 11 April 2003*)

Abstract. The disaster information system, the Early Damaged Area Estimation System (EDES), was developed to estimate damaged areas of natural disaster using the night-time imagery of the Defense Meteorological Satellite Program Operational Linescan System (DMSP-OLS). The system employs two estimation methods to detect the city lights loss or reduction as possible impacted areas; one is the bi-temporal images (BTI) method and the other is the time-series images (TSI) method. Both methods are based on significance tests assuming that brightness of city lights fluctuates as normal random variables, and the BTI method is simplified by introducing the assumption that the standard deviation of city lights fluctuation is constant. The validity of the estimation method is discussed based on the result of the application to the 2001 Western India earthquake disaster. The estimation results identify the damaged areas distant from the epicentre fairly well, especially when using the TSI method. The system is designed to estimate the global urban damage and to provide geographic information through the Internet within 24 h after a severe disaster event. The information is expected to support the disaster response and relief activities of governments and non-governmental organizations.

1. Background and objectives

In a severe natural disaster, spatial information of afflicted areas is indispensable to decision makers. Especially in the case of an earthquake, emergency and rescue activities should be mobilized promptly to appropriate places even if people in

International Journal of Remote Sensing
ISSN 0143-1161 print/ISSN 1366-5901 online © 2004 Taylor & Francis Ltd
http://www.tandf.co.uk/journals
DOI: 10.1080/01431160310001595033

destructive areas cannot ask for them because of malfunction of communication systems. Satellite remote sensing, which observes a wide area, can play an active part for this demand, and attracts considerable attention with recent high-performance sensors, e.g. very high resolution sensors and hyper-spectral sensors.

Remote sensing has been employed extensively to monitor flood, forest fire, volcano and geotechnical hazards (table 1) as well as weather, e.g. clouds, rain, snow, etc. While there have been a large number of remote sensing studies of disaster management, most of them aimed at monitoring hazards. In addition, the number of studies on urban damage detection is still limited. As for the adopted methods, optical sensor imagery is used to detect spectral changes brought about by a disaster, and infrared imagery is often considered for phenomena with thermal change, e.g. volcanic activities. With regard to the method with radar, Synthetic Aperture Radar (SAR) imagery is often used to detect backscattering change and a SAR interferogram is also consulted for events involving surface elevation change.

To extract details of urban damage, Inanaga *et al.* (1995) and Yoshie and Tsu (1995) examined the 1995 Hyogo-ken Nanbu earthquake using optical sensors. Matsuoka *et al.* (2001) conducted a quantitative analysis based on the detailed data of the building and proposed a damage detection method using Landsat Thematic Mapper (TM) and Système Pour l'Observation de la Terre High Resolution Visible imaging system (SPOT-HRV) imagery observed before and after the event (bi-temporal images). In that research, brightness changes differently in non-damaged areas, liquefaction areas, burnt areas, and damaged building areas, and the classification result based on a maximum likelihood method corresponds mostly to the damage survey data. Yonezawa and Takeuchi (2001) suggested that severely damaged areas can be extracted based on correlation analysis using European Remote Sensing Satellite (ERS) SAR imagery acquired before and after the earthquake. Matsuoka and Yamazaki (2001) discussed backscattering characteristics using the ERS SAR imagery, and developed a method to detect hard-hit areas based on linear discriminant analysis using difference and correlation of intensity as explanatory variables. André *et al.* (2002) used high-resolution satellite images of IKONOS and KVR 1000 to detect buildings that had been damaged by an earthquake.

Previous remote sensing research on urban damage detection has aimed mainly at identifying structural damage. But it should be recognized that the substance of a disaster is influential to human activities. To give an actual example, some floods cause vast economic loss due to communication and transportation problems even though there are few severely damaged buildings. In a modern city, which is highly dependent on widely extended lifelines, a short blackout could affect social and

Table 1. Hazard monitoring using satellite remote sensing in previous literature (except weather monitoring).

Hazard	Case study literature
Flood	Wiesnet *et al.* (1974), Imhoff *et al.* (1987), etc.
Forest fire	Tanaka *et al.* (1983), Robinson (1991), etc.
Volcano lava and fume	Rothery *et al.* (1988), Holasek and Rose (1991), etc.
Active lahars (volcanic mudflows)	Chorowicz *et al.* (1997)
Landslides	Saraf (2000), Kimura and Yamaguchi (2000), etc.
Ground deformation caused by an earthquake or volcanic activities	Massonnet *et al.* (1993), etc.

economic activities seriously. This type of indirect damage should not be ignored because it can potentially influence the world economy.

On the other hand, night-time urban city lights are correlated with energy consumption, population and various human activities, and some remote sensing studies have been done using Defense Meteorological Satellite Program Operational Linescan System (DMSP-OLS) imagery, as cited in the next section. Hence, the night-time image has possibility to detect disaster influence to human activities including indirect damage.

Although most of the past studies describe the image processing methods to detect damage, very few attempts have been made to discuss comprehensive information processing: acquisition of satellite images, processing the images to estimate damage, and disseminating the results for emergency response, or to develop a consistent system for global disaster management.

This paper introduces a near real-time global disaster information system using DMSP-OLS night-time imagery, which has been developed by the Earthquake Disaster Mitigation Research Center, National Research Institute for Earth Science and Disaster Prevention (EDM/NIED) of Japan and NOAA National Geophysical Data Center (NOAA/NGDC) of USA. The system, Early Damaged Area Estimation System (EDES), is designed to provide geographic information on possible impacted areas in order to support disaster relief activities of governments and non-governmental organizations. The estimation method used here is based on a new approach of probabilistic evaluation of night-time city lights. Regarding natural disasters, the EDES mainly deals with an earthquake disaster, in which emergency response is required. EDES is expected to assist response activities since there still exist a great number of disaster-prone countries without a disaster information system, e.g. a damage estimation system based on densely deployed seismic observation network.

2. DMSP-OLS remote sensing for disaster management

2.1. *Remote sensing research using DMSP-OLS night-time imagery*

Although DMSP-OLS has a lower spatial resolution (2.7 km at nadir) than that of SPOT-HRV or Landsat TM, its wide swath (2960 km) and frequent observation (repeat period of 1 day) are a great advantage in disaster monitoring. The OLS consists of two telescopes and a photo multiplier tube; one telescope acquires imagery in the visible and near-infrared (VNIR) band, which the photo multiplier tube enables to detect faint VNIR emission sources, and the other the thermal infrared (TIR) band. If there is no cloud influence, DMSP-OLS can observe disaster areas within 24 h. Foster (1983a) noted snow coverage, forest fire, lava, gas flare, city lights, etc. as the phenomena detectable in DMSP-OLS night-time imagery. Because city lights reflect the existence of human activities, many researchers have analysed the correlation between observed city lights and economic activities. Nakayama *et al.* (1993) showed the relation between the diameter of city lights and population and electricity consumption. Elvidge *et al.* (1997a) created the Stable Lights Image (SLI), which depicts stable city lights, processing multi-temporal images from October 1994 to March 1995. With this synthesized image, Elvidge *et al.* (1997b) indicated that lit areas correlate closely with population, gross domestic product, and electricity consumption. Some quantitative analyses also have been done with SLI: Sutton (1997), Nakayama (1998) and Konami *et al.* (1998) evaluated populations in USA, Japan and China, respectively. Furthermore, Sutton *et al.* (2001) estimated the global population.

The gain of OLS usually changes along with the elevations of the sun and the moon because the primary mission of DMSP is weather observation; the gain is controlled to acquire consistent cloud images. Elvidge *et al.* (1999) requested that the US Air Force fix the OLS gain setting of the retired DMSP/F12 to three different levels: 24, 40 and 50 dB from March 1996 to February 1997, and created a Radiance Calibrated Image (RCI). While a digital number (DN) of SLI represents the statistical probability of exceeding a threshold in a night-time image observed in a low moon period, the DN of RCI corresponds to radiance of physical quantity; RCI distinguishes light intensity even in the centre of cities, where DN of SLI saturates. Elvidge *et al.* (1999) demonstrated that the RCI has a higher correlation with population and electricity consumption in the USA than SLI, and Nakayama and Elvidge (1999) surveyed the correlation with the population in Hokkaido, Japan, and Lo (2001) proposed a population estimation model for China using the RCI.

With respect to forest fire, Elvidge *et al.* (1995) developed the fire detection algorithm to discriminate non-stationary lights apart from city lights by using SLI. Currently, NOAA/NGDC provides this estimation product and Elvidge *et al.* (2001) report the monitoring results of forest fire in Brazil. Nagano *et al.* (1998) proposed a prompt and wide-area monitoring method using DMSP-OLS night-time images and smoke images observed by the Geostationary Meteorological Satellite (GMS). Forestry and Forest Products Research Institute *et al.* (2001) developed the early fire detection system using images of DMSP-OLS and NOAA Advanced Very High Resolution Radiometer (NOAA AVHRR) in a project called ANDES (Asia Pacific Network for Disaster Mitigation using Earth Observation Satellite). The system automatically produces and archives fire location maps indicating both the hotspots in the TIR imagery of NOAA AVHRR and new lights in night-time imagery of DMSP-OLS every night.

As for snow cover and flood monitoring, Foster (1983b) pointed out that snowy regions reflect moonlight well and can be monitored by its area change based on the DMSP-OLS night-time image. But the DMSP Special Sensor Microwave/Imager (SSM/I), the microwave radiometer, is more often used to monitor sea ice (Cavalieri 1991, EOSDIS National Snow and Ice Data Center 1996, etc.), snow cover (Grody and Basist 1996, Standley and Barrett 1999, etc.) and flood areas (Jin 1999, Tanaka *et al.* 2000, etc.) because SSM/I can observe the moisture level of the ground surface.

With regard to urban damage detection, NOAA/NGDC (Elvidge *et al.* 1998) applied the forest fire detection method and proposed a detection method of power outage area, in which lights disappear even though stable lights were observed in SLI. But further discussions are required to determine the threshold to detect brown out rather than black out. In this paper, the newly proposed methods define the threshold as a significance level of a significance test.

2.2. *Earthquake influence on city lights observed by DMSP-OLS*

Most of the research on information acquisitions in an earthquake disaster have been aimed at detection of ground deformation or structural damage. But damage brought about by an earthquake include not only social stock damage, e.g. bridge damage, building collapse, etc., but also social flow damage, e.g. malfunctions of lifelines such as electricity, water, gas, communication or transportation. As city lights are figuratively used as a symbol of prosperity, a light emitter represents the

existence of human activity, e.g. room lights, street lights, advertisement lights, and the light intensity can be assumed to be an index of level of human activity. Therefore, a region where it becomes darker after an earthquake than at normal times can be considered to have suffered damage. Because city lights are mostly generated from electricity, the possible causes can be listed as shown in table 2.

The intensity of city lights observed by satellites fluctuates even at normal times due to the many factors shown in table 3. Among them, clouds greatly influence city lights observation. With respect to moonlight, if the area of the bright part and the elevation of the moon are almost the same, the influence can be assumed to be negligible when two images are compared. Long-term urban change should contribute little to the fluctuation when the studied period is within several months. When DMSP-OLS observes city lights, the further following points in table 3 should be considered as factors of fluctuation.

With respect to geolocation accuracy, Kohiyama *et al.* (2001) propose an accuracy-improving technique using RCI as a template of optimum position, and the sub-pixel accuracy is achieved. Pixel offset discrepancy causes serious influence to light change analysis when the comparison is based on images that are resampled

Table 2. Possible causes of loss of city lights.

Damage type	Possible causes
Structural damage	Damage of a power plant or automatic/manual halt of power plant after detection of strong motion.
	Controlled power supply caused by degraded capacity of power supply system.
	Damage of power line, substation or power receiver.
	Damage of light source (e.g. street light).
	Building collapse.
Social damage	Injury or death of residents.
	Evacuation of residents.
	Suspension or slowdown of commercial and business activities.

Table 3. Factors causing fluctuation of city lights intensity observed by satellites at normal times.

Satellites	Fluctuation factors
Observed by general satellites	• Atmospheric scattering and absorption.
	• Reflection and scattering of far city lights and moonlight by clouds.
	• Moonlight reflecting on ground surface.
	• Long-term city light change (city growth or decline).
	• Non-stationery light source (vehicle lights, room lights, switching signal lights, etc.).
Observed by DMSP-OLS	• Intensity change of direct and reflecting lights due to the difference of observation angle.
	• Change in travelling distance of lights through the atmosphere due to the difference of observation angle (atmospheric absorption).
	• Difference of instantaneous field of view from nadir to edge of swath.
	• Sensor measurement error of OLS.
	• Geolocation error.
	• Pixel offset discrepancy (centroid positions of pixels differ depending on each observation).
	• Gain-setting difference of OLS.

to a smaller cell-size image. A technique using the smoothing filter to an image resampled by the nearest-neighbour method, or using interpolation methods like bi-linear or cubic convolution is also proposed to address this problem. As mentioned before, the gain setting of OLS changes depending on the moon condition. During low moon period when the moon does not appear in the sky, the gain is adjusted to its highest level. But for an observation on other days, the gain setting is controlled to keep a consistent image of clouds, which reflects moonlight. In the high moon period, the moon condition should be taken into account when two images are compared.

Due to the above factors, the observed intensity of city lights fluctuates even in normal periods. Therefore, when a probabilistically significant change (both increment and decrement) of intensity occurs, the region can be considered a possible impacted area, where the reduction might be brought by an earthquake disaster.

3. Damaged area estimation using DMSP-OLS night-time imagery

3.1. *Bi-temporal images method*

The estimation method used in EDES is based on the basic significance tests of brightness of city lights. Hereby, the following two assumptions are made:

1. In normal times, the radiance of city lights follows a Gaussian distribution when they are observed through little cloud.
2. The pixel DN of a VNIR image observed by DMSP-OLS is derived from city lights of an urban area only inside of the pixel perimeter.

Elvidge *et al.* (1999) illustrate the relation between gain setting, radiance and DN of a VNIR image as shown in figure 1, which is based on the pre-flight calibration of OLS on-board DMSP/F12. The graph gives the following equation, where gain setting, radiance and DN of VNIR image are G (dB),

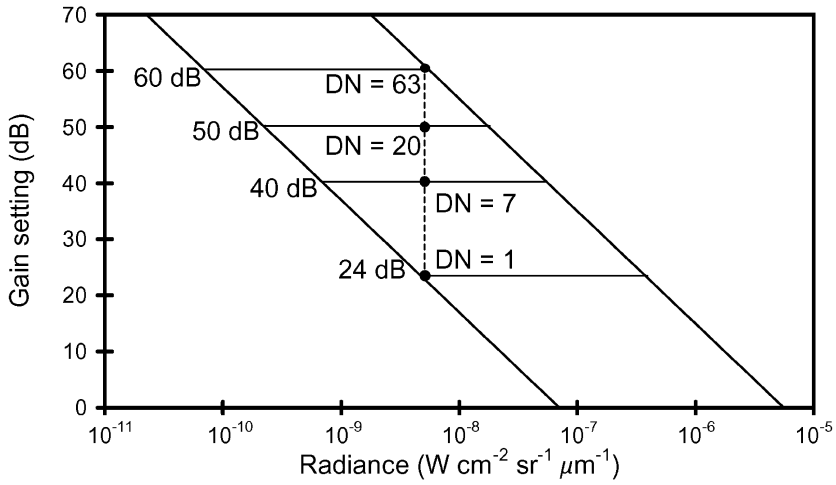

Figure 1. The relationship between gain setting, radiance and DN of a VNIR image (Elvidge *et al.* 1999).

R ($\mathrm{W\,cm^{-1}\,sr^{-1}\,\mu m^{-1}}$), D_V, respectively:

$$G = -20\log_{10} R + a\log_{10} D_V - C_1 (\mathrm{dB}) \tag{1}$$

$$R = 10^{-\frac{G+C_1}{20}} D_V^b \left(\mathrm{W\,cm^{-1}\,sr^{-1}\,\mu m^{-1}}\right) \tag{2}$$

$$D_V = 10^{\frac{G+C_1}{a}} R^{1/b} = 63^{\frac{G+C_1}{C_2}} R^{1/b} \tag{3}$$

$$\text{where } a = \frac{C_2}{\log_{10} 63} \approx 20.00,\ b \approx 1.000,\ C_1 = 141.83, \text{ and } C_2 = 35.99 \tag{4, 5, 6, 7}$$

The difference between DN of two VNIR images acquired in different times are given as follows:

$$\begin{aligned} \Delta D_V &= D'_V - D_V \\ &= 63^{\frac{G'+C_1}{C_2}} R'^{1/b} - 63^{\frac{G+C_1}{C_2}} R^{1/b} \\ &= C_3 \left(C_4^{G'} R'^{1/b} - C_4^G R^{1/b} \right) \end{aligned} \tag{8}$$

$$\text{where } C_3 = 63^{\frac{C_1}{C_2}} \approx 1.233 \times 10^7, \text{ and } C_4 = 63^{1/35.99} \approx 1.122. \tag{9, 10}$$

The gain settings are the same as G (dB), and equation (8) becomes:

$$\Delta D_V = 63^{\frac{G+C_1}{C_2}} \left(R'^{1/b} - R^{1/b} \right) = C_3 C_4^G \left(R'^{1/b} - R^{1/b} \right) \tag{11}$$

Because of equation (5) and the assumption (1), ΔD_V can be regarded as a normal random variable.

When two VNIR images are observed with different gain settings G, G', and DN of the same radiance are given D_V, D'_V, respectively, the equation (1) gives:

$$G' - G = a\log_{10} D'_V - a\log_{10} D_V = a\ \log_{10} \frac{D'_V}{D_V} (\mathrm{dB}), \text{ and} \tag{12}$$

$$D'_V = D_V 10^{\frac{G'-G}{a}} = D_V 63^{\frac{G'-G}{35.99}} \tag{13}$$

Consequently, a 6 dB gain difference gives approximately twice the DN, and 10 dB gives approximately three times.

Using the images of Taiwan Island acquired on 23 and 24 July 1999 (figures 2 and 3, respectively), a sample distribution of the differences between the DN of the two images is shown in figure 4. The pixels are selected to be in land, in urban areas with stable lights (DN of SLI is greater than zero) and with little cloud influence assuming that the temperature greater than 0°C does not correspond to heavy clouds based on the sea surface temperature. Total number of the pixels is 14 001. The mean and standard deviation of ΔD_V are -1.04 and 8.02, respectively. The histogram is similar to the Gaussian distribution with the mean and standard deviation, which is drawn in the same figure. The temperature θ (°C) is calculated based on DN of a TIR image:

$$\theta = \frac{310 - 190}{255} D_T + 190 - 273.15 \approx 0.4706\ D_T - 83.15\ (^\circ\mathrm{C}) \tag{14}$$

The fluctuation of city lights substantially differs depending on the scale of a

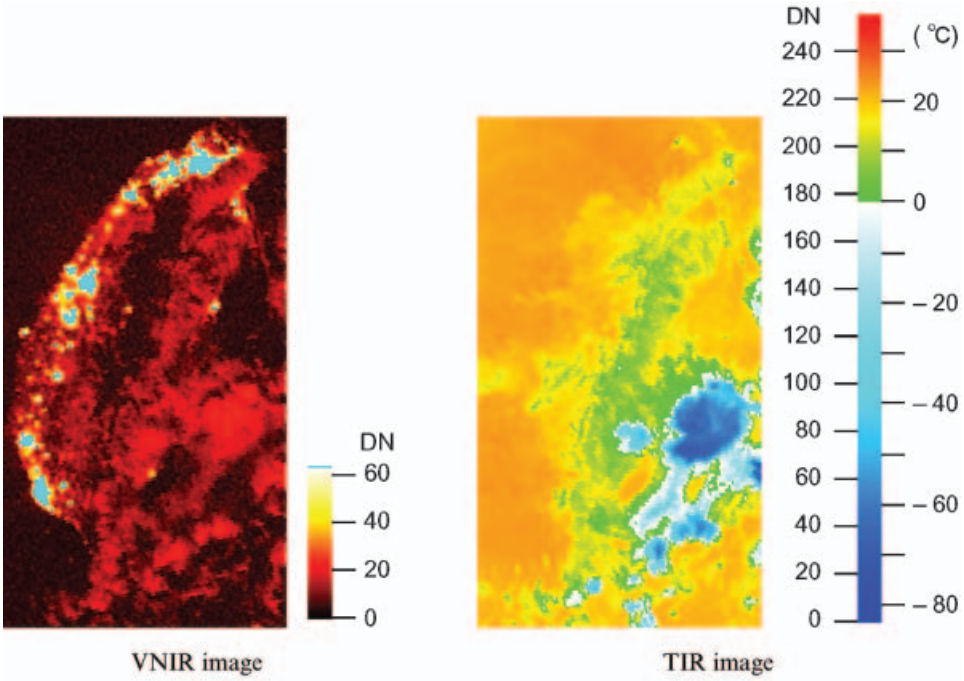

Figure 2. VNIR and TIR image of Taiwan island acquired on 23 July 1999 (image: F14199907231214).

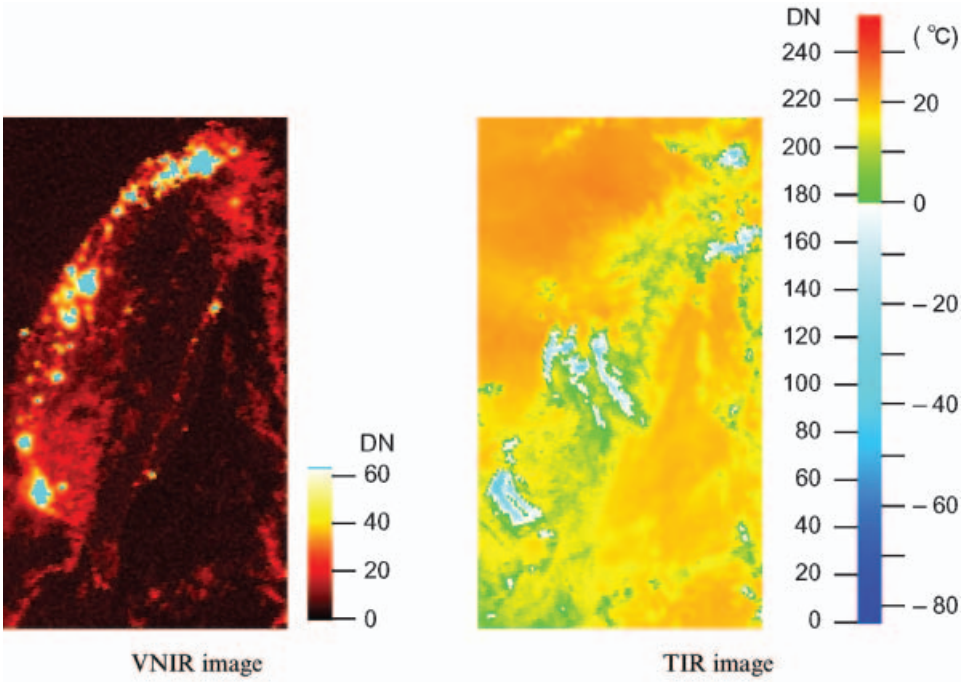

Figure 3. VNIR and TIR image of Taiwan Island acquired on 24 July 1999 (image: F14199907241202).

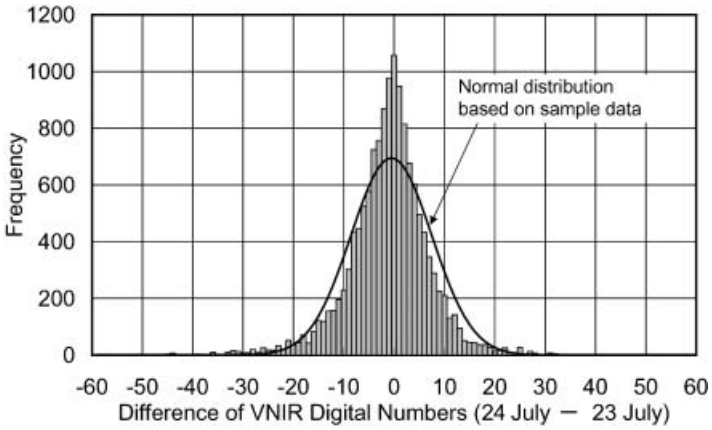

Figure 4. Histogram of digital number difference of the two visible near-infrared images in urban areas with little cloud influence.

city. But it requires statistically sufficient number of images to evaluate the fluctuation on a pixel basis, and it also requires long computer processing time to geolocate such a number of images. Therefore, the simple method, which evaluates city lights fluctuation based on only two images, should be practical, especially in urgent situation after a disaster. The following assumption is introduced for this purpose:

3. The fluctuation of radiance emitted from any urban area follows the same Gaussian distribution when it is observed by DMSP-OLS and the gain setting of OLS is the same.

This assumption enables measurement of the radiance fluctuation based on two images, but it is only valid for the images containing similar-scale cities. This assumed model will deviate from the real situation when the image contains different scales of residential areas, for a small village has dark city lights and consequently the absolute value of the fluctuation becomes small.

When a normal distribution of ΔD_V, the DN difference of bi-temporal images, is presumed, the pixels with a probabilistically significant reduction of DN can be statistically regarded as abnormal ones in which the radiance of city lights decreases abnormally departing from normal fluctuation in the area. To explain this, it can be stated another way: consider the null hypothesis:

> H_0: The fluctuation of DN of the VNIR image is in the Gaussian distribution in normal times (under conditions without any anomalous event, e.g. a disaster).

When H_0 is rejected by a critical region, the city lights reduction can be considered to be abnormal. If the two acquisition dates of images are before and after an earthquake, it is estimated that this significant reduction might be influenced by the earthquake and the area in the pixel could be a damaged area. The estimation process of the bi-temporal images (BTI) method is summarized as follows:

- Step 1: Select two images observed by DMSP-OLS before and after a disaster event with the following selection conditions: (1) The gain settings of the two

images are almost the same. (The gain difference should be less than 2 dB to avoid bias.) (2) The moonlight reflecting on the ground surface is almost the same (judging from the bright part of the moon and the moon elevation). (3) A target area contains enough undamaged area to evaluate the Gaussian distribution of city lights fluctuation in normal times. (4) The scales of cities in a target area can be regarded as uniform (judging from the DN histogram of the pre-event image).

- Step 2: Evaluate the mean and standard deviation of the normal distribution of DN differences between the two images assuming uniformity of city light fluctuation.
- Step 3: Calculate a threshold of significance tests to dismiss H_0 based on the Gaussian distribution and a significance level (e.g. 95% or 99%).
- Step 4: Examine the DN differences on a pixel basis based on a significance test of a Gaussian distribution and estimate if the pixel area is a possible impacted area or not.

In Step 3, thresholds of two significance levels, 95% and 99%, are calculated to classify damaged areas based on probabilities. In an estimation result map, possible impacted areas of 95% and 99% significance levels are coloured in yellow and red, respectively.

When a target area contains a large portion of damaged areas with considerable light reductions, the standard deviation, which is evaluated based on sample data in the target area, becomes larger than that of evaluation in normal times. Thus, in this case, the target areas should be enlarged in order to include sufficient pixels to evaluate normal fluctuation.

3.2. *Time-series images method*

The BTI method includes the following problems due to the introduced assumptions:

1. It is not easy to find a pre-event image without the influence of cloud scattering, reflecting and screening.
2. Water bodies reflecting city lights before an earthquake induce misdetection of damage.
3. The damage of comparatively smaller cities with weak lights tends to be neglected.

Optical sensors generally have the problem (a). The cloud-free image is preferred as a pre-event image. To avoid the influence of cloud in a pre-event image, Kohiyama *et al.* (2000a,b) proposed evaluating an artificial pre-event image based on SLI and RCI, respectively. The problems (b) and (c) come from the assumption that the city lights fluctuation is homogeneous in a target area, and it is necessary to evaluate each area fluctuation independently in order to address these problems. Otherwise, estimation results give biased information of damaged areas, neglecting small towns even though the estimation originally aims to support the unbiased disaster response activities.

Time-series analysis is available to evaluate a fluctuation of each area. Based on the fact that a VNIR image has little influence of moonlight in a gain stable period (about 10 days) of the darker part of the lunar cycle including new moon, a mean and a standard deviation of DN in each pixel can be calculated based on 3 months of data (total about 30 nights images). The DN can be converted into radiances

based on the gain estimation method mentioned above. Therefore, the time-series images (TSI) method is proposed, which employs significance tests on a pixel basis based on each Gaussian distribution with the mean and the standard deviation of DN in each pixel, as follows:

> Step 1: Select 3 months of images observed by DMSP-OLS before a disaster event in normal times with the following selection condition: images are observed in gain-stable periods in the darker parts of the lunar cycle with the same gain setting.
> Step 2: Evaluate means and standard deviations of the Gaussian distributions of DN on a pixel basis.
> Step 3: Calculate the threshold DN of significance tests based on the Gaussian distribution and levels of significance (e.g. 95% and 99%) on a pixel basis.
> Step 4: Examine radiances of a post-event on a pixel basis based on a significance test of a Gaussian distribution and estimate whether or not the pixel area is a possible impacted area.

This method can address not only problems (b) and (c), but also the problem (a) of cloud influence in a pre-event image because the probability should be very small that the same area is covered by clouds in all the pre-event images, except in continuously or seasonally cloudy (or foggy) areas. For all its advantages, the method has the following week points:

- The computer processing time is much longer than for the BTI method because a large number (about 30) of images are required.
- The gain estimation method (Kohiyama 2000b) and mean and standard deviation estimation in bright city light areas are highly dependent on RCI and the error will become large when the image acquisition date is a long way from the creation dates of RCI due to urban growth or decay.
- Images observed under moonlight should be compensated by considering the intensity of reflecting moonlight compared with that of city lights.

The TSI method should be very effective if RCI is updated using an adequate time interval; NOAA/NGDC has updated the RCI using the year 2000 data and sustains its efforts for the revision.

4. Application to the Western India earthquake of 26 January 2001

The Western India earthquake, which occurred at 8:46 26 January 2001 (local time) in Gujarat State, India near the boundary between India and Pakistan, caused destructive damage with large magnitude Mw 7.7 (US Geological Survey). The number of casualties exceeded 20 000, and Pakistan also experienced damage including more than ten casualties.

First, the BTI method is applied to estimate the damage. The image of 24 January 2001 is selected as a pre-event image because there is no image for 25 January 2001 covering the entire area around the epicentre. The VNIR and TIR images of pre-event and post-event (26 January 2001) are shown in figures 5 and 6, respectively. The lunar conditions at the acquisition times (table 4) suggest that both images are observed around new moon and have the same gain setting values.

Figure 7 is a histogram of DN difference between pre-event and post-event images with the ordinate of logarithmic scale. The estimated damaged areas based on the BTI method in figure 8 shows widely spread damaged areas; threshold 0°C is

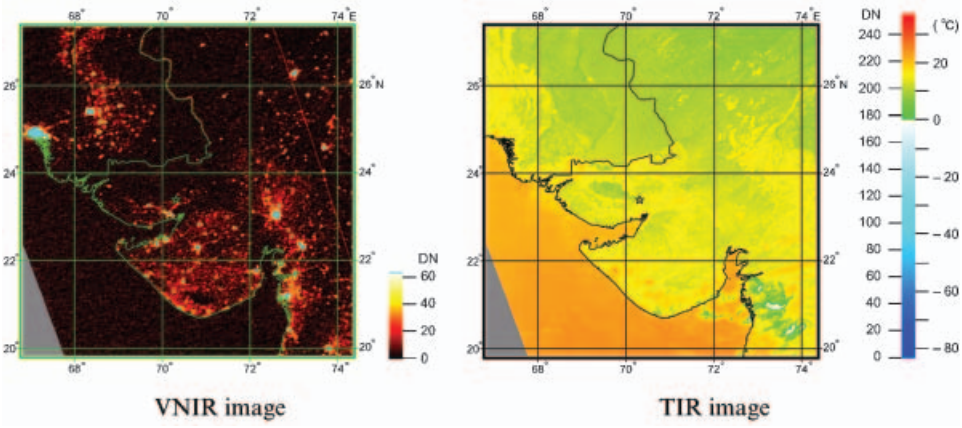

Figure 5. VNIR and TIR images of pre-event, 24 January 2001 (image: F15200101241539).

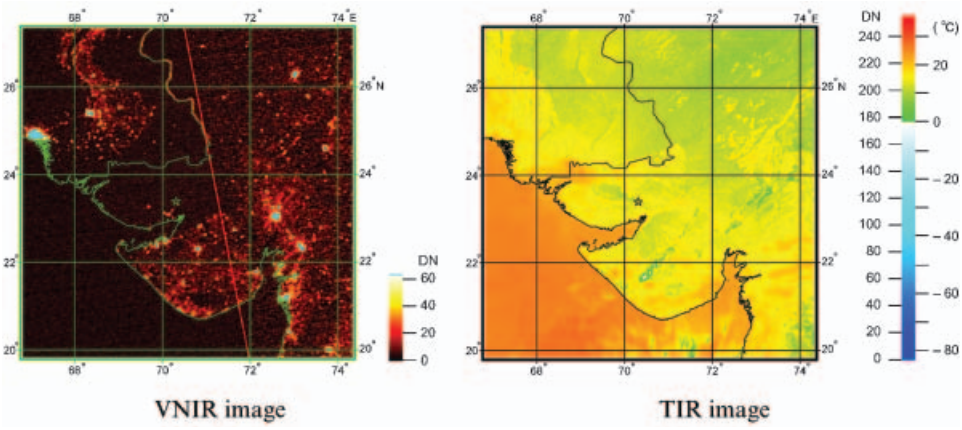

Figure 6. VNIR and TIR images of post-event, 26 January 2001 (image: F15200101261652).

Table 4. Lunar conditions at acquisition times.

DMSP-OLS image	Acquisition time	Lunar age (days)	% Bright area of the Moon
F15200101241539	21:16, 24 Jan 2001	0.1	0.0
F15200101261652	22:29, 26 Jan 2001	2.2	4.1

In the name of the DMSP-OLS image, 'FxxYYYYMMDDhhmm', xx, YYYY, MM, DD, hh and mm represent the satellite number, and year, month, day, hour and minute of the equator crossing time.

used for cloud screening and pixels with DN < 1 in SLI are masked in order to remove noise derived from lights other than city lights. However, considering the rivers on the map, the estimated damaged areas in annotated circles in the upper-left, upper and lower right parts are probably due to the unreliable data near swath edge, water reflection and both water reflection and cloud influence, respectively.

Secondly, the TSI method is applied with the same post-event image. A total of

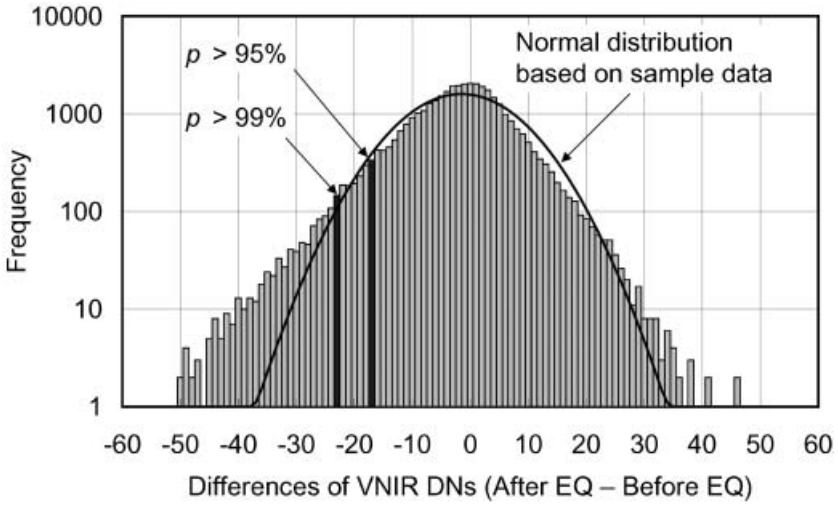

Figure 7. Histogram of DN difference between two VNIR images of pre-event and post-event; the ordinate is a logarithmic scale.

Figure 8. Map of areas damaged by the 2001 Western India earthquake estimated by the bi-temporal images method.

32 pre-event images are selected from images observed in darker part of lunar cycle from October 2000 to January 2001 before the earthquake as listed in table 5. The estimation result is shown in figure 9, where non-urban areas are masked using VNIR average image with threshold value: DN < 6 for noise removal; this mask preserves more pixels in small towns than the mask used in the BTI method. In figure 9, most of estimated damaged areas, which seem to be mis-detected in

Table 5. Pre-event images used for the time-series images method (32 images).

Month	DMSP-OLS image
October 2000	F15200010201630, F15200010211616, F15200010221602, F15200010231547, F15200010241533, F15200010251519, F15200010271632, F15200010281618, F15200010291604, F15200010301549, F15200010311535
November 2000	F15200011201555, F15200011211540, F15200011221526, F15200011241639, F15200011251625, F15200011271556, F15200011281542
December 2000	F15200012201532, F15200012211518, F15200012231631, F15200012241617, F15200012251602, F15200012261548, F15200012271534, F15200012281519, F15200012291647, F15200012301632
January 2001	F15200101201636, F15200101211622, F15200101231553, F15200101241539

Figure 9. Map of areas damaged by the 2001 Western India earthquake estimated by the time-series images method.

figure 8, are diminished and additional damaged areas appear in small towns owing to the estimation method and the mask difference.

The district damage statistics in Gujarat State are reported as shown in table 6 (Gujarat Informatics Limited, as of 5 and 28 February 2001); the districts map are shown in figure 10. The population, human loss and damaged buildings in Kachchh region (Murakami 2001) are shown in table 7. The estimated damaged areas coincide with them generally. The damage in the cities near the epicentre—Bhuj, Bachau and Anjar—are all well detected in the results of both estimation methods and these cities were actually severely damaged, as shown in table 7. The damage in Lakhpat County, where Panadra is located, is also indicated in both results even though it is 200 km from the epicentre; the collapse ratio of permanent (masonry) buildings in Lakhpat County is 16% and there exists actual damage, although most

Table 6. Damage statistics in Gujarat State for the 2001 Western India earthquake (Gujarat Informatics Limited, as of 5 and 28 February 2001).

	Date of information					
	As of 28 February 2001			As of 5 February 2001		
District	Number of affected talukas	Number of affected villages	Human deaths	Number injured	Houses/Huts collapsed	Houses/Huts damaged partially
Ahmedabad	11	392	751	4030	940	15 253
Amreli	11	273	0	5	585	8580
Anand	8	124	1	20	33	804
Banaskantha	8	452	32	2770	1849	8336
Bharuch	8	248	9	44	292	2864
Bhavnagar	11	535	4	44	1010	9906
Gandhinagar	4	210	8	240	2	913
Jamnagar	11	685	119	4 592	24 858	77 297
Junagadh	14	554	8	87	457	11 593
Kachchh	10	949	18 188	39 765	150 396	107 139
Kheda	10	350	0	28	72	690
Mehsana	9	611	0	1139	41	1004
Navsari	5	313	17	51	98	222
Patan	8	349	37	1686	13 707	31 302
Porbandar	3	157	9	90	2544	14 736
Rajkot	14	686	433	10 567	3682	20 522
Sabarkantha	8	68	0	56	1	84
Surat	8	94	46	157	21	860
Surendranagar	10	661	113	2851	28 256	85 329
Vadodra	6	85	1	256	62	104
Valsad	5	108	0	0	0	77
Total	182	7904	19 776	68 478	228 906	397 615

of the news media reported damage in Bhuj City near the epicentre soon after the earthquake. The estimation resulting from the BTI method is linked to a Web page on the day after the occurrence of the earthquake. If the information were successfully sent to the disaster managers, response activities might be changed.

5. Early damaged areas estimation system

The mortality rate of people demanding rescue becomes much higher when it passes 72 h after an occurrence of an earthquake. Lifesaving requires the promptest action in the response activities. The EDES is targeted to disseminate estimation results of damaged areas within 24 h of a severe natural disaster. DMSP-OLS imagery was restricted to be in public use after 72 h hold time, but the hold time was relaxed to 3 h on 20 December 1999 so that the EDES target is capable of being carried out.

Figure 11 shows the network diagram of EDES. Since 1992, NOAA/NGDC receives and archives digital DMSP-OLS images, which are sent from DMSP satellites via US Air Force. The DMSP-OLS images are mirrored and stored for 3 months in the EDES server placed in NOAA/NGDC. Currently, night-time images of two satellites sensors, DMSP/F14-OLS and DMSP/F15-OLS, are sent to the server so as to ensure the observation of target areas.

The estimation of damaged areas is ignited by a trigger e-mail that exceeds a preset threshold of magnitude of an earthquake. There are some e-mail services that

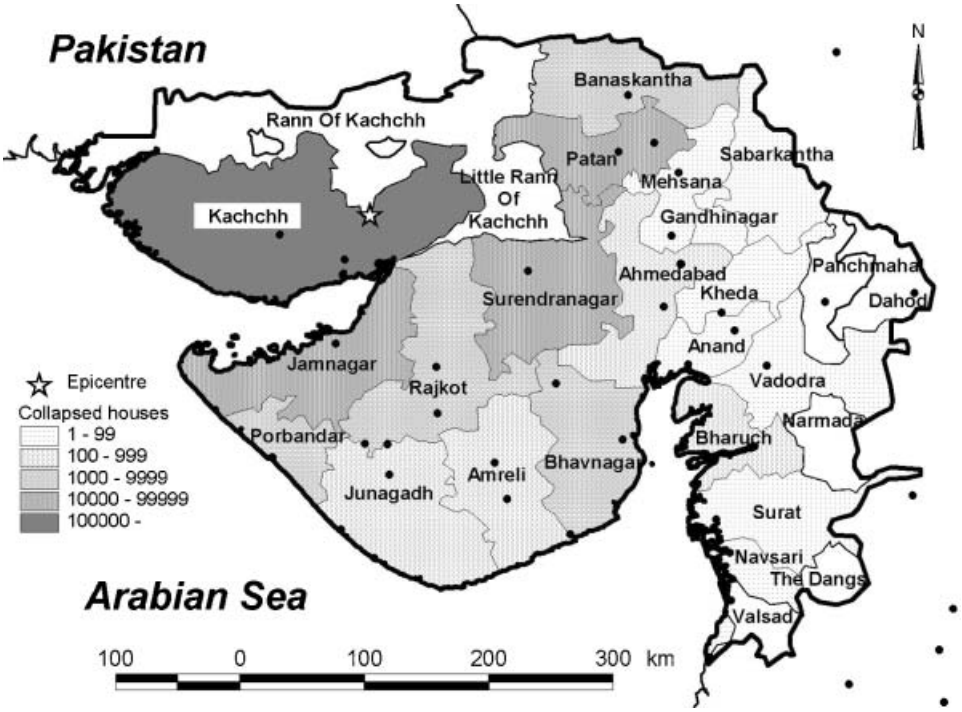

Figure 10. Map of districts in Gujarat State, India, and distribution of collapsed houses (table 6).

provide information on world earthquakes (occurrence time, hypocentre location and magnitude), e.g. BIGQUAKE of the US Geological Survey (USGS National Earthquake Information Center 2001); EDES parses the mail content of earthquake information. The direct command input by a staff administrator can activate estimation for other kinds of disasters. The final estimation results are linked to the World Wide Web servers in both NOAA/NGDC and EDM/NIED, and the results are also sent by e-mail based on a pre-registered mailing list. Figure 12 shows the process flow chart from receiving a trigger e-mail to disseminating the estimation result.

EDES monitors each disaster area for three nights after the onset of a disaster, as simple power outage tends to be recovered comparatively quickly and severely damaged areas with structural damage would remain as a dark city in the second or third day. In addition, one would expect to acquire a cloud-free image in three nights. The optical sensor has the disadvantage that heavy clouds influence its images; DMSP-OLS is the first platform and sensor that EDES implements. Other sensor images are in the scope of future plan and SAR is promising to overcome this disadvantage.

6. Conclusions

A near real-time information system for disaster mitigation, the EDES, has been developed using DMSP-OLS night-time imagery. The system provides the geographic information for damaged areas, which are useful for disaster response activities, especially in developing countries. The estimation is based on the reduction or loss of city lights that falls outside of normal fluctuation. Two

Table 7. Population, human loss and damaged buildings in the Kachchh region (Murakami 2001).

Taluka (county) name	Households	1991 Population	No. of dead	Death rate (%)	Collapsed pucca (masonry) ratio (%)	Collapsed kuchcha (adobe) ratio (%)	Epicentral distance (km)
Bhuj	55 486	277 215	4503	1.62	57	67	68
Mundra	13 945	68 652	65	0.09	77	85	85
Mandvi	27 876	146 034	72	0.05	49	83	118
Abdasa	17 070	86 402	19	0.02	22	23	152
Lakhpat	7416	36 759	2	0.01	16	8	162
Nakhatrana	21 610	116 944	23	0.02	12	26	108
Rapar	24 273	150 517	732	0.49	69	91	38
Bachau	22 944	114 759	7424	6.47	95	95	12
Anjar*	32 176	160 640	4702	2.93	77	81	43
Gandhidham†	20 743	104 585	861	0.82	45	54	43
Total	243 539	1 262 507	18 403	1.46	59	63	

*Anjar Taluka except for Gandhidham
†Gandhidham city area.

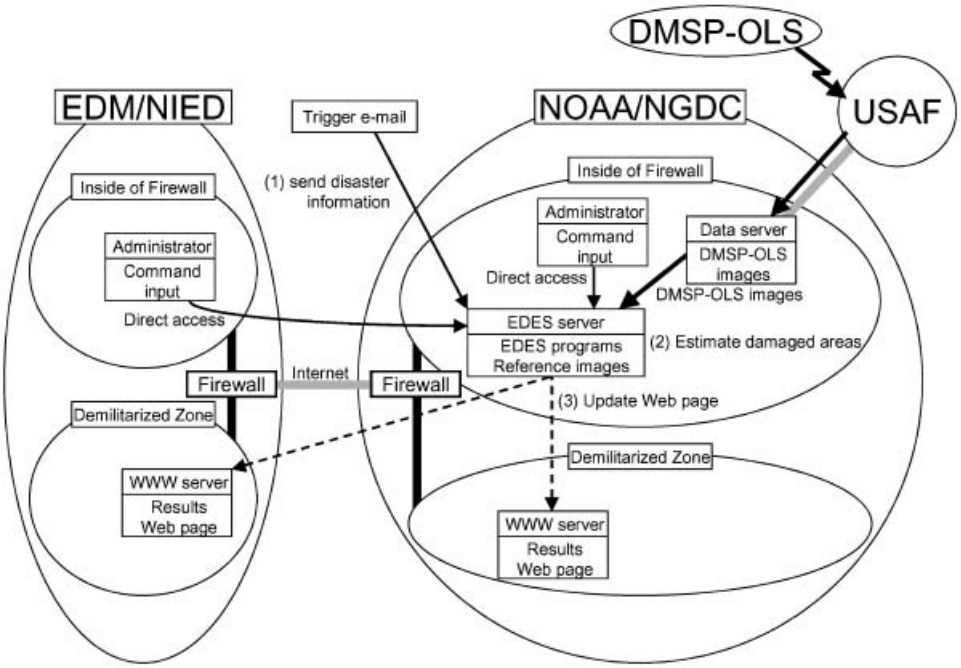

Figure 11. Network diagram of the EDES.

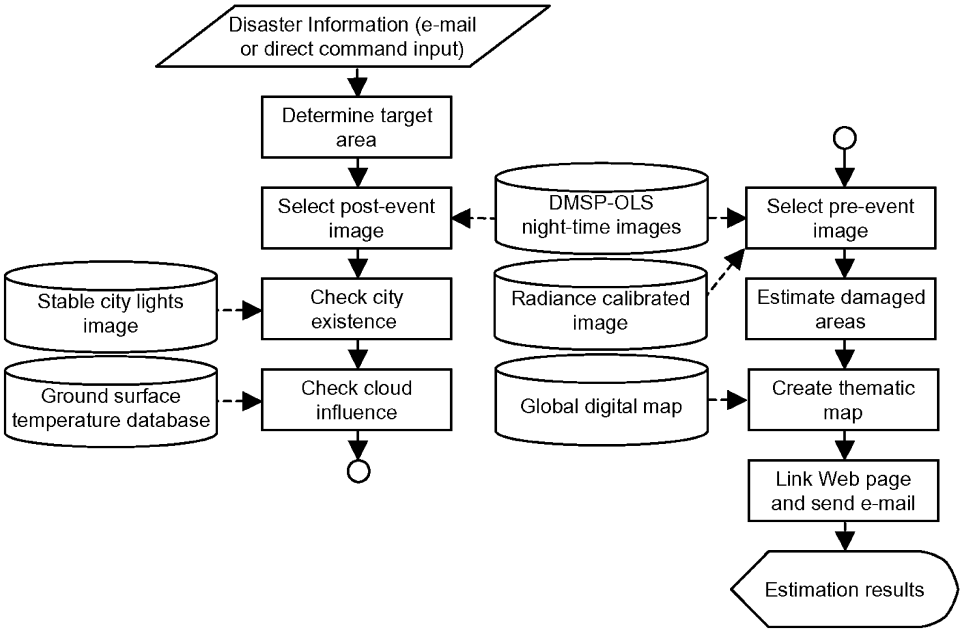

Figure 12. Process flow chart of the EDES from receiving the trigger e-mail to dissemination of the result.

methods, the bi-temporal images method and the time-series images method are proposed, and these use two images acquired before and after a disaster event, and time-series images, respectively. Both methods are based on the assumption that

radiances of city lights fluctuate as normal random variables. The estimation methods are applied to the 2001 Western India earthquake, and its validity is discussed. The result supports its capability in disaster mitigation in addition to the previous application results of the 1995 Hyogo-ken Nanbu (Kobe), Japan, the 1999 Kocaeli, Turkey, and the 1999 Chi-Chi, Taiwan earthquakes (Kohiyama *et al.* 2000a, b, 2001).

The estimation methods can be applied for images from other kinds of sensors for change detection. That means the methods are applicable for the next generation of satellites, e.g. National Polar-orbiting Operational Environmental Satellite System Visible/Infrared Imager/Radiometer Suite (NPOESS-VIIRS). The estimation accuracy will be improved by using the new sensors because of their wider dynamic range and geolocation accuracy.

The present EDES employs only DMSP-OLS imagery, but all types of data should be utilized for disaster management. There are various kinds of remotely sensed images such as SAR and the hyper-spectral optical sensor, and insisting upon one sensor image is not wise. For example, an earthquake-triggered fire gives a misdetection of damaged areas using EDES, but that can be overcome by using a thermal–infrared image observed by a higher resolution sensor like that of NOAA. It is necessary to establish the framework to turn multiple sensor images to practical use for the future system. Furthermore, a disaster information system should support decision makers, and further functions, such as rescue deployment and material allocation for disaster victims, are required. The system should be expanded in order to provide a holistic information system.

Acknowledgments

Development of the EDES was conducted as a joint research project of the National Oceanic and Atmospheric Administration, National Geophysical Data Center (NOAA/NGDC) and the Earthquake Disaster Mitigation Research Center, National Research Institute for Earth Science and Disaster Prevention (EDM/NIED). The DMSP-OLS images, Stable City Lights Image, and Radiance Calibrated Image were provided by NOAA/NGDC. DMSP-OLS images of India were distributed through the Ministry of Agriculture, Forestry and Fisheries Research Network's Satellite Image Database System in the Ministry of Agriculture, Forestry and Fisheries (MAFFIN-SIDaB) (Kodama and Song 2000). The authors would like to acknowledge the generosity of these organizations.

References

André, G., Chiroiu, L., Guillande, R., and Galaup, M., 2002, Evaluation et cartographie de dommages par imagerie satellite SPOT 5: simulation sur la ville de Bhuj, séisme du Gujurat, Inde (26 janvier 2001). *Bulletin de la Société Française de Photogrammétrie et Télédétection*, **164/165**, 174–183.

Cavalieri, D. J., 1991, NASA sea ice validation program for the Defense Meteorological Satellite Program Special Sensor Microwave Imager. *Journal of Geophysical Research*, **96**, 21969–21970.

Chorowicz, J., Lopez, E., Garcia, F., Parrot, J.-F., Rudant, J.-P., and Vinluan, R., 1997, Keys to analyze active lahars from Pinatubo on SAR ERS Imagery. *Remote Sensing of Environment*, **62**, 20–29.

Elvidge, C. D., Kroehl, H. W., Kihn, E. A., Baugh, K. E., Davis, E. R., and Hao, W. M., 1995, Algorithm for the retrieval of fire pixels from DMSP Operational Linescan System data. In *Global Biomass Burning*, edited by J. S. Levine (Cambridge, Massachusetts: MIT Press), pp. 73–85.

Elvidge, C. D., Baugh, K. E., Kihn, E. A., Kroehl, H. W., and Davis, E. R., 1997a,

Mapping city lights with nighttime data from the DMSP Operational Linescan System. *Photogrammetric Engineering and Remote Sensing*, **63**, 727–734.

ELVIDGE, C. D., BAUGH, K. E., KIHN, E. A., KROEHL, H. W., DAVIS, E. R., and DAVIS, C. W., 1997b, Relation between satellite observed visible-near infrared emissions, population, economic activity and electric power consumption. *International Journal of Remote Sensing*, **18**, 1373–1379.

ELVIDGE, C. D., BAUGH, K. E., HOBSON, V. R., KIHN, E. A., KROEHL, H. W., and KROEHL, H. W., 1998, Detection of fires and power outages at night using DMSP-OLS data, Internet file as of 19 November 1998, http://www.ngdc.noaa.gov/dmsp/fires/fires_desc.html.

ELVIDGE, C. D., BAUGH, K. E., DIETZ, J. B., BLAND, T., SUTTON, P. C., and KROEHL, H. W., 1999, Radiance calibration of DMSP-OLS low-light imaging data of human settlements. *Remote Sensing of Environment*, **68**, 77–88.

ELVIDGE, C. D., HOBSON, V. R., BAUGH, K. E., DIETZ, J. B., SHIMABUKURO, T. E., KRUG, T., NOVO, E. M. L. M., and ECHAVARRIA, F. R., 2001, DMSP-OLS estimation of tropical forest area impacted by surface fire in Roraima, Brazil: 1995 versus 1998. *International Journal of Remote Sensing*, **22**, 2661–2673.

EOSDIS NATIONAL SNOW AND ICE DATA CENTER, 1996, *DMSP SSM/I Brightness Temperatures and Sea Ice Concentration Grids for the Polar Regions*. User's Guide (Boulder, Colorado: NSIDC, University of Colorado).

FOSTER, J. L., 1983a, Observations of the earth using nighttime visible imagery. *Proceedings of Society of Photo-optical Instrumentation Engineers*, **414**, 187–193.

FOSTER, J. L., 1983b, Night-time observations of snow using visible imagery. *International Journal of Remote Sensing*, **4**, 785–791.

FORESTRY AND FOREST PRODUCTS RESEARCH INSTITUTE, METEOROLOGICAL RESEARCH INSTITUTE, NATIONAL SPACE DEVELOPMENT AGENCY, NATIONAL INSTITUTE OF AGRICULTURAL ENVIRONMENT STUDY, COMPUTER CENTER FOR AGRICULTURE, FORESTRY AND FISHERIES RESEARCH, AND JAPAN SCIENCE AND TECHNOLOGY CORPORATION, 2001, Asia-Pacific network for disaster mitigation using earth observation satellite (ANDES). Research Report, Forestry and Forest Products Research Institute, Japan.

GRODY, N. C., and BASIST, A. N., 1996, Global identification of snowcover using SSM/I measurements. *IEEE Transactions on Geoscience and Remote Sensing*, **34**, 237–249.

GUJARAT INFORMATICS LIMITED, 2001, Details of Affected Districts. Internet file as of 5 and 28 February 2001, http://www.gujaratinformatics.com/quake/district_details.html.

HOLASEK, R. E., and ROSE, W. I., 1991, Anatomy of 1986 Augustine volcano eruptions as recorded by multispectral image processing of digital AVHRR weather satellite data. *Bulletin of Volcanology*, **53**, 429–435.

IMHOFF, M. L., VERMILLION, C., STORY, M. H., CHOUDHURY, A. M., GAFOOR, A., and POLCYN, F., 1987, Monsoon flood boundary delineation and damage assessment using space borne imaging radar and Landsat data. *Photogrammetric Engineering and Remote Sensing*, **53**, 405–413.

INANAGA, A., TANAKA, S., TAKEUCHI, S., TAKASAKI, K., and SUGA, Y., 1995, Remote sensing data for investigation of earthquake disaster. *21st Annual Conference of the Remote Sensing Society*, *11–14 September 1995* (Nottingham: Remote Sensing Society), pp. 1089–1096.

JIN, Y. Q., 1999, A flooding index and its regional threshold value for monitoring floods in China from SSM/I data. *International Journal of Remote Sensing*, **20**, 1025–1030.

KIMURA, H., and YAMAGUCHI, Y., 2000, Detection of landslide areas using satellite radar interferometry. *Photogrammetric Engineering and Remote Sensing*, **66**, 337–343.

KODAMA, M., and SONG, X., 2000, A new remote sensing database system in Ministry of Agriculture, Forestry and Fisheries, Japan. *51st International Astronautical Congress* (Paris: International Astronautical Federation), IAF-00-B.4.05, pp. 1–11.

KOHIYAMA, M., HAYASHI, H., MAKI, N., HASHITERA, S., MATSUOKA, M., KROEHL, H. W., ELVIDGE, C. D., and HOBSON, V. R., 2000a, Development of Early Damaged Area Estimation System (EDES) using DMSP/OLS nighttime imagery. *Journal of the Institute of Social Safety Science*, **2**, 79–86 [in Japanese].

KOHIYAMA, M., HAYASHI, H., MAKI, N., and HASHITERA, S., 2000b, Validity study of EDES application to Taiwan Chi-Chi earthquake disaster. *21th Asian Conference on Remote Sensing* (Taipei: Center for Space & Remote Sensing Research, National

Central University, and Chinese Taipei Society of Photogrammetry and Remote Sensing), vol. 1, 407–412.

KOHIYAMA, M., HASHITERA, S., MAKI, N., and HAYASHI, H., 2001, Development of Early Damaged Area Estimation System using DMSP/OLS nighttime imagery. EDM Technical Report, No. 10, Earthquake Disaster Mitigation Research Center, Institute of Physical and Chemical Research, Japan [in Japanese].

KONAMI, T., SHIBASAKI, R., and TAN, G., 1998, Using nighttime DMSP-OLS images of citylights to estimate district-level population distribution in developing countries. *19th Asian Conference on Remote Sensing* (Manila: National Mapping and Resource Information Authority), pp. Q21_1–6.

LO, C. P., 2001, Modeling the population of China using DMSP Operational Linescan System nighttime data. *Photogrammetric Engineering and Remote Sensing*, **67**, 1037–1047.

MASSONNET, D., ROSSI, M., CARMONA, C., ADRAGNA, F., PELTZER, G., FEIGL, K., and RABAUTE, T., 1993, The displacement fields of the Landers earthquake mapped by radar interferometry. *Nature*, **364**, 138–142.

MATSUOKA, M., YAMAZAKI, F., and MIDORIKAWA, S., 2001, Characteristics of satellite optical images in areas damaged by the 1995 Hyogo-ken Nanbu earthquake. *Journal of Structural Mechanics and Earthquake Engineering, Japan Society of Civil Engineering*, **668/I-54**, 177–185 [in Japanese].

MATSUOKA, M., and YAMAZAKI, F., 2001, Characteristics of satellite SAR intensity images in building damage areas due to the 1995 Hyogo-ken Nanbu earthquake. *Journal of Structural and Construction Engineering, Architectural Institute of Japan*, **546**, 55–61 [in Japanese].

MURAKAMI, H., 2001, Outline of damage survey. A comprehensive survey of the 26 January 2001 earthquake (Mw7.7) in the State of Gujarat, India. Report by the research team supported by the grant-in-aid for specially promoted research provided by the Japanese Ministry of Education, Culture, Sports, Science and Technology in the fiscal year of 2000, Grant No. 12800019, Japan, pp. 51–55.

NAGANO, O., YAMAMOTO, H., OKADA, Y., HONDA, Y., KAJIWARA, K., and ELVIDGE, C. D., 1998, Study of monitoring method for huge forest fire using DMSP and GMS. *Journal of the Japanese Society of Photogrammetry and Remote Sensing*, **37**, 32–41 [in Japanese].

NAKAYAMA, Y., TANAKA, S., and SUGA, Y., 1993, DMSP global nighttime image and its geographical meanings. *Journal of the Remote Sensing Society of Japan*, **13**, 1–14 [in Japanese].

NAKAYAMA, M., 1998, DMSP-OLS imagery to estimate population. *International Symposium on Resource and Environmental Monitoring* (Budapest: Technical Com VII, International Society for Photogrammetry and Remote Sensing), pp. 1–4.

NAKAYAMA, M., and ELVIDGE, C. D., 1999, Applying newly developed calibrated radiance DMSP-OLS data for estimation of population. *20th Asian Conference on Remote Sensing* (Hong Kong: Joint Laboratory for GeoInformation Science of The Chinese Academy of Sciences and The Chinese University of Hong Kong), vol. 1, pp. 289–293.

ROBINSON, J. M., 1991, Fire from space: global fire evaluation using infrared remote sensing. *International Journal of Remote Sensing*, **12**, 3–24.

ROTHERY, D. A., FRANCIS, P. W., and WOOD, C. A., 1988, Volcano monitoring using short wavelength infrared data from satellites. *Journal of Geophysical Research*, **93**, 7993–8008.

SARAF, A. K., 2000, IRS-1C-PAN depicts Chamoli earthquake induced landslides in Garhwal Himalayas, India. *International Journal of Remote Sensing*, **21**, 2345–2352.

STANDLEY, A. P., and BARRETT, E. C., 1999, The use of coincident DMSP SSM/I and OLS satellite data to improve snow cover detection and discrimination. *International Journal of Remote Sensing*, **20**, 285–305.

SUTTON, P., 1997, Modeling population density with night-time satellite imagery and GIS. *Computers, Environment, and Urban Systems*, **21**, 227–244.

SUTTON, P., ROBERTS, D., ELVIDGE, C., and BAUGH, K., 2001, Census from heaven: an estimate of the global human population using night-time satellite imagery. *International Journal of Remote Sensing*, **22**, 3061–3076.

TANAKA, S., KIMURA, H., and SUGA, Y., 1983, Preparation of a 1:25 000 Landsat map for

assessment of burnt area on Etajima Island. *International Journal of Remote Sensing*, **4**, 17–31.

TANAKA, M., SUGIMURA, T., and TANAKA, S., 2000, Monitoring water surface ratio in the Chinese floods of summer 1998 by DMSP-SSM/I. *International Journal of Remote Sensing*, **21**, 1561–1569.

USGS NATIONAL EARTHQUAKE INFORMATION CENTER, 2001, Earthquake Notification Services: Bigquake. Internet file as of 7 May 2001, http://wwwneic.cr.usgs.gov/neis/data_services/data_services.html.

WIESNET, D. R., MCGINNIS, D. F., and PRITCHARD, J. A., 1974, Mapping of the 1973 Mississippi River floods by NOAA-2 satellite. *Water Resources Bulletin*, **10**, 1040–1049.

YOSHIE, T., and TSU, H., 1995, A satellite data processing to delineate the densely built-up areas damaged disastrously by 1995 Hyogoken-nanbu earthquake. *18th Japanese Conference of Remote Sensing* (Tokyo: Remote Sensing Society of Japan), pp. 119–122 [in Japanese].

YONEZAWA, C., and TAKEUCHI, S., 2001, Decorrelation of SAR data by urban damages caused by the 1995 Hyogoken-nanbu earthquake. *International Journal of Remote Sensing*, **22**, 1585–1600.